arXiv:1303.6241v1 [physics.soc-ph] 25 Mar 2013

# Structure of complex networks: Quantifying edge-to-edge relations by failure-induced flow redistribution

**Michael T. Schaub[1], Jörg Lehmann[2], Sophia N. Yaliraki[3] and Mauricio Barahona[1]**

[1] Department of Mathematics, Imperial College London, London SW7 2AZ, U.K.
[2] ABB Switzerland Ltd, Corporate Research, CH-5405 Baden-Dättwil, Switzerland
[3] Department of Chemistry, Imperial College London, London SW7 2AZ, U.K.

E-mail: michael.schaub09@imperial.ac.uk, m.barahona@imperial.ac.uk

**Abstract.** The analysis of complex networks has so far revolved mainly around the role of nodes and communities of nodes. However, the dynamics of interconnected systems is commonly focalised on edge processes, and a dual edge-centric perspective can often prove more natural. Here we present graph-theoretical measures to quantify edge-to-edge relations inspired by the notion of flow redistribution induced by edge failures. Our measures, which are related to the pseudo-inverse of the Laplacian of the network, are global and reveal the dynamical interplay between the edges of a network, including potentially *non-local* interactions. Our framework also allows us to define the embeddedness of an edge, a measure of how strongly an edge features in the weighted cuts of the network. We showcase the general applicability of our edge-centric framework through analyses of the Iberian Power grid, traffic flow in road networks, and the *C. elegans* neuronal network.

PACS numbers: 02.50.Ga, 88.80.hh, 89.75.-k, 89.75.Fb

Submitted to: *New J. Phys.*

## 1. Introduction

The use of network formulations for the analysis of complex systems has attracted tremendous interest over the last years. Network-centric approaches, in which the entities (agents, particles) of a system are represented as nodes in a graph and their interactions are denoted by (weighted, directed, multiplex) edges between nodes, have been successfully employed to model biological, technical and social systems [1–3]. The trend towards adopting a network perspective has also been facilitated by the increased availability of large relational datasets and growing computational resources. Inevitably, this data-driven approach has led to the generation of large, highly complex networks. However, such networks have limited explicative power and further analysis is usually needed to extract relevant representations from such complex annotation of system interactions. In this context, a key driver has been the area of *community detection*, which aims at providing coarse-grained, simplified descriptions of a network based on groups of nodes (i.e., communities) in order to provide insight about the structure and function of the overall system [4, 5].

Thus far, the vast majority of research on complex networks has been naturally focused on nodes, their roles, and their groupings into meaningful communities. However, in a number of scenarios it is the dynamics on the edges and their interplay that defines the behaviour of the system. Consider the generic case in which the edges carry a flow (signal, data, mass, energy, etc), and where fluctuations or failures (total or partial) on the edges can occur or be induced. If the (direct) path between nodes A and B is blocked and only a fraction of the intended flow can be transmitted, this can cascade through the network affecting the flow on other links. In this case, *edge variables* and their mutual influences constitute the object of interest in the modeling. Specifically, we consider here the *coupling between edges* induced by flow redistribution; how to relate this edge-to-edge coupling to properties of the graph; and how to uncover potentially long-range relations between edges. Such an analysis has not been pursued, although graph-theoretical notions such as the *line graph*, which records the immediate adjacency of edges, are well known [6, 7] and have been used to investigate overlapping communities in networks [8, 9].

In the following, we introduce a framework to quantify edge-to-edge relations based on the dynamics of linear flow and its redistribution under perturbations to the network. Our analysis borrows notions from electrical networks and its classic analogy to a random walk description [10]. In particular, we derive edge-to-edge relationships inspired by the so called *line-outage distribution factor* in electrical networks and show how this factor can be decomposed into two measures with concrete graph-theoretical interpretations. These measures enable us to quantify the influence between edges and the likelihood of edges to be critical to the redistribution of flow in the network. Our derivation relates these notions explicitly to generic graph properties which can be readily calculated from associated matrices of the graph to reveal features in the organisation of complex networks, thus making our concepts applicable to a variety of systems.

## 2. Linear flows, electrical networks and random walks

*Notation*

We consider connected, weighted, undirected graphs with $N$ nodes (or vertices) and $E$ edges (or links). Each edge $e$ is endowed with an arbitrary (but fixed) 'reference' direction that points from the tail node $t(e)$ to its head $h(e)$. Note that the graph is still *undirected*, i.e., flow is allowed to pass in both directions along each edge and the reference direction merely specifies the sign of the flow on the edge. Each edge $e$ is associated with a $N \times 1$ incidence vector $\mathbf{b}_e$ with entries $[b_e]_{h(e)} = -1$, $[b_e]_{t(e)} = 1$ and zero otherwise. Note that other authors use the opposite sign convention for $\mathbf{b}_e$. The node-to-edge incidence matrix can then be written as:

$$B_{N\times E} = [\mathbf{b}_1 \cdots \mathbf{b}_E].$$

Each edge $e$ has an associated weight (or conductance) $g_e$, which we compile into a diagonal matrix

$$G_{E\times E} = \mathrm{diag}(g_e). \tag{1}$$

The *(weighted) graph Laplacian* or *Kirchoff conductance matrix* $L$ is then:

$$L_{N\times N} = \sum_{e=1}^{E} g_e \mathbf{b}_e \mathbf{b}_e^T = BGB^T. \tag{2}$$

For connected, undirected graphs, $L$ is symmetric positive semidefinite, with a simple zero eigenvalue and corresponding eigenvector $\mathbf{1}$, the vector of ones [11, 12].

### *2.1. Linear flows on networks and electrical quantities*

A large class of network processes can be modeled by linear dynamics on a network, described by state variables on the nodes and edges of a graph (c.f. the book by Strang [13] for an insightful discussion and the reformulation of diverse problems in these terms). Systems of this type include widely used models of spring-mass-damper networks of mechanical systems, as well as electrical networks and reversible Markov chains (i.e., random walks or diffusion processes on undirected networks), among many others. In all cases, a constitutive relation links the flow along an edge with the node variables at its tail and head. The simplest such relation is an Ohm-type law that establishes a linear relationship between the flow on the edge and the difference between the associated node variables. This dual edge-node description is at the heart of applications in circuit theory (even with nonlinear elements [14, 15]), computational mechanics, estimation theory, as well as Systems Engineering and primal/dual problems in optimisation theory. The edge formulation can be exploited to highlight the relevance of processes focalised on the edges (or the cycles) rather than on the nodes of the network [13].

To make our formulation of embedded linear processes clearer, we introduce the framework through the canonical example of electrical resistor networks [13, 16] and its well-known connection with random walks [10]. We remark that electrical resistor

networks are not only relevant for electrical engineering applications, such as power systems, but can be seen as archetypal models for linear processes and, as such, are of interest in various biological applications (e.g., vision [17,18]) or in the area of community detection [19].

Henceforth, node variables are denoted by capital letters, while small letters are reserved for edge quantities. In a resistor network, the flows on the edges correspond to electrical currents driven by potential differences across the edges, as given by Ohm's law. Each node $k$ in the network has an associated potential $V_k$ and the potential difference over edge $e$ is $v_e = V_{t(e)} - V_{h(e)}$. Given the vector of node potentials $\mathbf{V}$, the vector of voltages across the edges is: $\mathbf{v} = B^T\mathbf{V}$. The current on each edge is equal to the edge voltage times the conductance:

$$\mathbf{i} = GB^T\mathbf{V} \quad \text{(Ohm's law)}. \tag{3}$$

Furthermore, by Kirchoff's current law (KCL), the in- and out-flow of currents at each node is balanced:

$$B\mathbf{i} = \mathbf{I}_{ext} \quad \text{(Kirchhoff's current law)}, \tag{4}$$

where $\mathbf{I}_{ext}$ is the vector of external currents injected into the nodes. ‡

The properties of the incidence matrix $B$ are directly connected with certain physical constraints. First, the vector of ones $\mathbf{1}_{N\times 1}$ is in the nullspace of $B^T$, consistent with KCL. Hence $\mathbf{1}^T\mathbf{I}_{ext} = 0$ and the net injected current into the system must be zero. Second, the nullspace of $B$ is the cycle space [7,16], i.e., the space spanned by all cycle vectors. Any (oriented) cycle in the graph can be represented by a vector $\mathbf{c}_{E\times 1}$ as follows: moving along the edges in the cycle, $c_e = 1$ if the edge direction is aligned with the direction of the cycle and $c_e = -1$ if it is opposite, with all other entries of $\mathbf{c}$ zero. Then for any cycle, $\mathbf{c}^T\mathbf{v} = \mathbf{c}^TB^T\mathbf{V} = 0$, i.e., the voltage drop around any cycle in the graph must be zero §. This is of course Kirchhoff's voltage law (KVL).

Combining (3) and (4), we get the well-known network equations relating input currents and node voltages:

$$L\mathbf{V} = \mathbf{I}_{ext}. \tag{5}$$

Using standard nodal analysis [13], we must first solve for the potential of the nodes $\mathbf{V}$ in (5) and then obtain the edge currents from (3). Equation (5) can always be solved, though not uniquely since $L$ is singular. This corresponds to the fact that the node potentials have an arbitrary reference. To fix a reference, the network is commonly *grounded*, i.e., the potential of one (arbitrary) node is set to zero. This leads to the definition of a $(N-1)$-dimensional *grounded Laplacian matrix* obtained by deleting a row and the corresponding column [20,21].

‡ If external voltage sources $\mathbf{v}_{ext}$ along the edges are present, then $\mathbf{i} = G(B^T\mathbf{V} - \mathbf{v}_{ext})$. However, we do not need to consider external voltage sources separately since each external voltage source can be transformed into its equivalent current source (Norton equivalent)

§ If magnetic fields need to be included in this formulation, they would be represented by additional current/voltage sources.

An alternative way of obtaining a unique $\mathbf{V}$ from (5) is through the Moore-Penrose pseudoinverse of the Laplacian, $L^\dagger$, which can be written as [22]:

$$L^\dagger = \left(L + \frac{1}{N}\mathbf{1}\mathbf{1}^T\right)^{-1} - \frac{1}{N}\mathbf{1}\mathbf{1}^T. \tag{6}$$

The particular vector of node potentials (and the corresponding edge currents) are then obtained as:

$$\mathbf{V} = L^\dagger \mathbf{I}_{ext} \tag{7}$$

$$\mathbf{i} \;\; = GB^T L^\dagger \mathbf{I}_{ext}. \tag{8}$$

It is well known that the $\mathbf{V}$ in (7) is the solution of (5) with minimal $L_2$ norm, and $\mathbf{V}^T\mathbf{1} = 0$. Hence the node potentials obtained have zero mean, i.e., the voltages are referred to the average potential [21].

### *2.2. Effective resistances and random walk interpretations*

An important property in electrical networks is the effective resistance $R_{ij}$ between two nodes $i$ and $j$. Physically, $R_{ij}$ is the potential drop measured when a unit current is injected at node $i$ and extracted at node $j$. The effective resistance can be compactly written in terms of the Laplacian pseudoinverse as [22]:

$$R_{ij} = (\mathbf{U}_i - \mathbf{U}_j)^T L^\dagger (\mathbf{U}_i - \mathbf{U}_j), \tag{9}$$

where $\mathbf{U}_i$ is the $i$-th unit vector, with a one at the $i$-th coordinate and zeros in all other coordinates. Clearly, $R_{ij} = R_{ji}$. The effective resistance defines a distance metric on the graph [23] and is also commonly known as the *resistance distance* (between two nodes). For a detailed overview and additional interpretations of this quantity see Ref. [22] and references therein. Note that $R_{ij}$ has a global dependence on the network as it takes into account all possible paths between $i$ and $j$. Therefore, even if nodes $i$ and $j$ are directly connected by an edge with conductance $g_e$, the effective resistance $R_{ij}$ will *not* in general be equal to $1/g_e$. This effect, induced by the presence of the network , underpins the concepts developed below.

A broader, alternative perspective on the electrical formalism discussed above is provided by the theory of harmonic functions on a graph, which establishes a fundamental relationship between electrical networks and reversible random walks on a graph. Detailed accounts of this topic are given in the books of Doyle and Snell [10] and Aldous and Fill [24], amongst others. In the context of random walks, the resistance distance is shown to be proportional to $T_{ij}$, the commute time of a random walker between nodes $i$ and $j$ [22, 24, 25]:

$$R_{ij} = \frac{T_{ij}}{2\,\mathrm{trace}(G)}, \tag{10}$$

where $T_{ij}$ is the expected time for a random walker to return to node $i$ for the first time after starting from node $i$ and passing through node $j$.

The random walk picture also provides interpretations for the currents and voltages [10]. Let a unit current be injected into node $i$ and extracted at node $j$. Then the current $\mathrm{i}_e$ corresponds to the net expected number of times a random walker which starts at node $i$ and walks until she reaches $j$ will cross edge $e$ in the defined orientation. On the other hand, voltages can be interpreted as relative hitting probabilities. Let a unit voltage be applied between nodes $i$ and $j$. Then the potential at node $k$ corresponds to the probability that a random walker starting from $k$ will hit node $i$ first before reaching $j$.

## 3. Edge-to-Edge relationships based on flow redistribution

### *3.1. The flow-redistribution matrix*

The characterisation of how edges influence each other on a network appears naturally in electrical networks such as the power grid. In such networks, it is important to assess the effect that the failure of one edge would have on other edges in terms of the extra redistributed flow that other edges must carry. Such an effect is quantified through the so-called *line outage distribution factor* [26]. We now introduce this concept through a graph-theoretical formulation and construct an edge-to-edge matrix, the *flow-redistribution matrix* that contains all such edge dependencies. The properties of the this edge-to-edge matrix reflect fundamental characteristics of the network structure.

Consider a resistor network with weighted Laplacian $L$ and external current injection/extraction $\mathbf{I}_{ext}$. The node voltages $\mathbf{V}$ and edge currents $\mathbf{i}$ can be obtained through (7)–(8). Consider now a line outage event: an edge $f$ fails and the flow redistributes through the network (see Figure 1a). The redistributed flow can be calculated easily as follows. The Laplacian matrix $\widehat{L}_f$ of the new network after the failure of edge $f$ is:

$$\widehat{L}_f = L - g_f \mathbf{b}_f \mathbf{b}_f^T. \tag{11}$$

Applying a generalised version of the Sherman-Morrison-Woodbury formula to the pseudoinverse [27], the new voltages are:

$$\widehat{\mathbf{V}} = \widehat{L}_f^\dagger \mathbf{I}_{ext} = \left( L^\dagger + \frac{L^\dagger \mathbf{b}_f g_f \mathbf{b}_f^T L^\dagger}{1 - g_f\, \mathbf{b}_f^T L^\dagger \mathbf{b}_f} \right) \mathbf{I}_{ext}. \tag{12}$$

The change in the node potentials is then:

$$\Delta_f \mathbf{V} = (\widehat{L}_f^\dagger - L^\dagger)\mathbf{I}_{ext} = \frac{L^\dagger \mathbf{b}_f g_f \mathbf{b}_f^T L^\dagger}{1 - g_f\, \mathbf{b}_f^T L^\dagger \mathbf{b}_f} \mathbf{I}_{ext}. \tag{13}$$

Note that $\mathrm{i}_f$, the current on edge $f$ *before* its failure, is:

$$\mathrm{i}_f = g_f v_f = g_f \mathbf{b}_f^T \mathbf{V} = g_f \mathbf{b}_f^T L^\dagger \mathbf{I}_{ext}. \tag{14}$$

Using (8) and (13)–(14), the $E \times 1$ vector of changes in the edge currents when edge $f$ fails can be written as:

$$\Delta_f \mathbf{i} = \left[ \frac{G B^T L^\dagger \mathbf{b}_f}{1 - g_f\, \mathbf{b}_f^T L^\dagger \mathbf{b}_f} \right] \mathrm{i}_f \equiv \mathbf{k}_f\, \mathrm{i}_f, \tag{15}$$

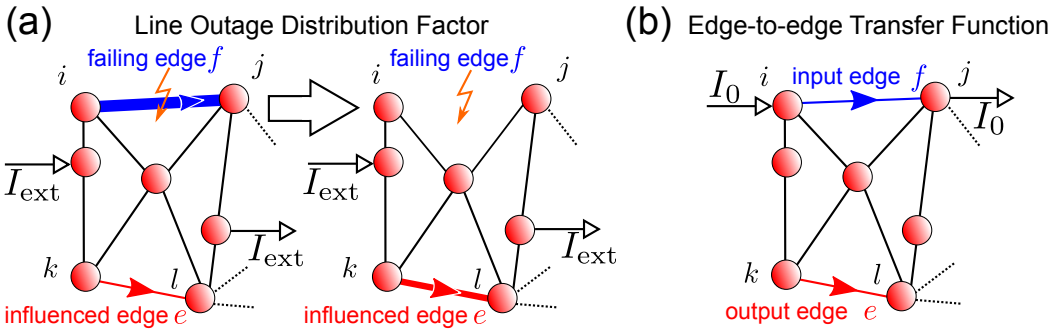


**Figure 1.** Schematic description of the line outage distribution factor (columns of the flow-redistribution matrix) and the edge-to-edge transfer function. (a) Line outage distribution factor: a line failure of edge $f$ will influence the flow on other edges in the network, as illustrated here for edge $e$. (b) Edge-to-edge transfer function: an ideal unit current injection along an edge $f$ induces flows in the network, as depicted here for edge $e$.

In the electrical engineering literature, the vector $\mathbf{k}_f$ is called the *line outage distribution factor* for edge $f$. Intuitively, the line outage distribution factor is a measure of the *edge-to-edge* dependency in terms of the flow redistribution following an edge failure. Note that $\mathbf{k}_f$ is *independent* of the injected current pattern $\mathbf{I}_{ext}$.

If we examine the effect of each of the $E$ edges failing in turn, we get the corresponding vectors $\mathbf{k}_i$, which we assemble into the *flow-redistribution matrix*:

$$K_{E\times E} \equiv [\mathbf{k}_1 \cdots \mathbf{k}_E], \tag{16}$$

which describes the edge-to-edge sensitivity under all possible single edge failures. Since the flow redistribution matrix is independent of the particular current injection, $K$ describes a *topological property* of the system, namely the edge-to-edge influence under a perturbation of the flows on the links.

We remark that the $f$-th component of $\Delta_f\mathbf{i}$ in (15) (and hence the diagonal entries of $K$) does not correspond to the (trivial) change in current on the failed edge. We will show below that these entries convey information which can be directly related to structural properties of the failing edge.

### *3.2. Decomposing the flow redistribution matrix: edge-to-edge transfer function and edge embeddedness*

Further insight into the interpretation of the flow redistribution matrix can be gained by noticing that it can be factorised as the product of two matrices with specific graph-theoretical meaning.

Consider a network with weighted Laplacian $L$ and assume we inject and extract a current $I_0$ at the tail and head of an edge $f$, i.e., $\mathbf{I}_{ext} = I_0\mathbf{b}_f$ (see Figure 1b). Equation (8) shows that such an injection/extraction of current across edge $f$ induces the following current flows in the rest of the network:

$$\mathbf{i}_{[f]} = \left[GB^TL^\dagger\mathbf{b}_f\right] I_0 \equiv I_0\,\mathbf{m}_f. \tag{17}$$

The edge vector $\mathbf{m}_f$ is a so called transfer function relating the injection/extraction of the current $I_0$ at edge $f$ to the currents induced on all other edges. The matrix compiling all transfer function vectors is the *edge-to-edge transfer function matrix*:

$$M_{E\times E} \equiv [\mathbf{m}_1 \cdots \mathbf{m}_E] = GB^T L^\dagger B, \tag{18}$$

and $M_{ef}$ describes how a unit current 'input' at edge $f$ is translated into a current 'output' at edge $e$. Note that, using (15), we can rewrite (17) in terms of the line outage distribution factor vector $\mathbf{k}_f$:

$$\mathbf{i}_{[f]} = I_0 \left[1 - g_f \mathbf{b}_f^T L^\dagger \mathbf{b}_f\right] \mathbf{k}_f \equiv I_0 \, \varepsilon_f \, \mathbf{k}_f, \tag{19}$$

where we have introduced the *edge embeddedness*, $\varepsilon_f$.

With these definitions, the flow-redistribution matrix can be rewritten as

$$K = M \left[\mathrm{diag}(\boldsymbol{\varepsilon})\right]^{-1}, \tag{20}$$

where $\boldsymbol{\varepsilon}$ is the vector of edge embeddednesses ‖.

The matrices $K$ and $M$ and the vector $\boldsymbol{\varepsilon}$ constitute the main object of our work and the means through which we study edge-to-edge relations. We now present in detail some properties of the edge-to-edge transfer function matrix and edge embeddedness.

*3.2.1. The edge-to-edge tranfer function matrix* The edge-to-edge tranfer function matrix $M$ is an interesting object in its own right. The matrix $M$ can be be regarded as a discrete Green's function on the edge space of the graph and appears in other contexts in graph theory (e.g., graph sparsification [28]).

Graph-theoretically, $M$ defines an orthogonal projection onto the *weighted cut space* of the graph (see Appendix). The weighted cut space, defined as the range of $GB^T$, establishes the linear combinations of weighted edge vectors that disconnect the network. Note from (20) that the weighted cut space is also the column space of the flow-redistribution matrix $K$ (provided no edge has zero embeddedness). The action of $M$ can thus be given a purely graph-theoretical interpretation: it finds the projection of an 'input' edge current (or combinations of those) onto the space of weighted cuts, thus allowing us to evaluate how much of the input current gets distributed onto current patterns associated to the weighted cuts disconnecting the network.

$M$ can also be understood in terms of effective resistances and commute times. Consider edge $e$ linking nodes $i$ and $j$, and edge $f$ linking nodes $k$ and $l$. From (18) and the definitions (9) and (10), it follows that:

$$\begin{aligned} M_{ef} &= g_e(L^\dagger_{ik} - L^\dagger_{il} + L^\dagger_{jl} - L^\dagger_{jk}) \\ &= \frac{g_e}{2}(R_{jk} - R_{ik} + R_{il} - R_{jl}) \qquad (21) \\ &= \frac{\pi_e}{4}\left((T_{jk} - T_{ik}) + (T_{il} - T_{jl})\right) \qquad (22) \end{aligned}$$

‖ We remark that the line outage distribution factor (and hence the flow-redistribution matrix) is undefined for edges with zero embeddedness. As will be become clear in section 3.2.2 however, if such an edge fails, the effect can be trivially understood by considering the related subgraphs independently. Hence, we only consider examples in which the flow-redistribution matrix is well defined.

where $(T_{jk} - T_{ik})$ is the difference of commute times to nodes $i$ and $j$ when starting from node $k$, and $(T_{il} - T_{jl})$ is the difference of commute times to nodes $i$ and $j$ when starting from node $l$. Here, $\pi_e = g_e/\text{trace}(G)$ is just the probability of a random walker crossing edge $e$ (in any direction) at stationarity in the original network. From this point of view, the edge-to-edge transfer function compares the difference in commute times to the two nodes of the 'output' edge $e$ as observed from the two nodes of the 'input' edge $f$. A similar formula to (21) for the flow-redistribution matrix $K$ can also be given [29].

The flow-redistribution matrix ($K$) and the edge-to-edge transfer function matrix ($M$) are closely yet subtly related. While $M$ describes how a current fed into an edge translates into currents at all edges, the flow-redistribution matrix describes the relative dependency of edge flows under edge failure. To understand their relationship, one can show that the edge-to-edge transfer function appears naturally when we consider the flow-redistribution matrix of a partial *$\alpha$-line failure* defined as follows. Assume that instead of encountering a complete failure of edge $f$, its conductance is only reduced by $\alpha g_f$ with $\alpha \in [0, 1]$. From (11), the Laplacian after such a line failure is $\widehat{L}_f(\alpha) = L - \alpha g_f \mathbf{b}_f \mathbf{b}_f^T$. Assuming the same scalar factor $\alpha$ applies to all edges, the flow-redistribution matrix for the $\alpha$-line failure is:

$$K(\alpha) = \alpha M \left[I - \alpha \,\text{diag}(M_{ee})\right]^{-1}. \tag{23}$$

For small $\alpha$, this expression can be linearised to give:

$$\begin{aligned} K(\alpha) &\approx K(0) + \left.\frac{dK(\alpha)}{d\alpha}\right|_{\alpha=0} \alpha \\ &= 0 + M\left[I - \alpha\,\text{diag}(M_{ee})\right]^{-2} \Big|_{\alpha=0} \alpha = \alpha M. \end{aligned} \tag{24}$$

Therefore $M$ is the slope with which small conductance fluctuations at each edge affect the flow on the other edges.

*3.2.2. The edge embeddedness* The embeddedness (19) of edge $e$ can be rewritten as:

$$\varepsilon_e = 1 - g_e \mathbf{b}_e^T L^\dagger \mathbf{b}_e = 1 - M_{ee} = 1 - g_e R_e, \tag{25}$$

where $M_{ee}$ is the corresponding diagonal element of $M$ and $R_e \equiv R_{h(e)t(e)}$ is the resistance distance (9) between the two endpoints of edge $e$. Expression (25) makes again clear that the resistance distance along an edge, $R_e$, is generally not the same as its local, 'physical' resistance, $r_e = 1/g_e$. In fact, the edge embeddedness measures how close $R_e$ and $r_e$ are.

It is well known from Rayleigh's Monotonicity law [10] that $R_e \leq r_e$, with equality only if edge $e$ is part of no cycle in the graph, i.e., if $e$ accounts for the only path between $t(e)$ and $h(e)$. Indeed, $R_e$ can always be written as the local resistance $r_e$ in parallel to a resistance $R_{\text{rest}}$ stemming from the rest of the network:

$$\frac{1}{R_e} = \frac{1}{R_{\text{rest}}} + \frac{1}{r_e}. \tag{26}$$

Intuitively, $R_{\text{rest}}$ will be small if the network has many alternative paths (i.e. cycles) with low resistance connecting $h(e)$ and $t(e)$. Hence for $\varepsilon_e$ to be large, edge $e$ participates in

many cycles of short weighted length, i.e., it is highly 'embedded.' On the other hand, a small $\varepsilon_e$ indicates that the edge participates in few cycles of small weight in the network. Therefore, such an edge has a major influence on the induction of cuts in the network and is key in providing a connection that keeps the network connected.

In terms of random walks, (22) and (25) allow us to write the embeddedness of an edge $e$ with tail node $i$ and head node $j$ as:

$$\varepsilon_e = 1 - \pi_e \frac{T_{ij}}{2} = 1 - \frac{T_{ij}}{2\tau_e}, \tag{27}$$

where $\tau_e$ is the expected time for a random walker to return to edge $e$. Thus the embeddedness compares the expected return time of a random walker to an edge and the commute time between the two edge endpoints.

The following interpretations of the embeddedness *valid for unweighted graphs* are also worth noting briefly. In the unweighted case, the embeddedness of an edge is the probability that the edge is not found in a spanning tree selected randomly with uniform probability ¶. For an unweighted graph, $M$ is symmetric and idempotent (A.1) and $M_{ee}$ is equal to the squared $L_2$ norm of the columns of $M$ [28]. Hence, $\varepsilon_e$ provides a measure of how global the influence of a current injection along edge $e$ is.

## 4. Using edge-to-edge relations for network analysis

We now use the flow-redistribution matrix, edge-to-edge transfer function matrix and edge embeddedness defined above to characterise the edge-to-edge properties of networks. To aid us in our network-theoretic analysis, we draw upon tools from community detection. Specifically, we use the recent method of *Markov stability of graph communities* [30–32] to find relevant groupings of edges according to their influence on each other as measured by the flow-redistribution matrix. The stability method is particularly useful for our purposes since it intrinsically scans across scales, thus enabling the detection of a broad range of communities, including long-range or non clique-like structures that can escape detection by other commonly used methods [33, 34].

### *4.1. Application to a simple constructive example: a ring of small-worlds*

To illustrate our analysis, consider a network of $N = 150$ nodes in which 5 small-world [35] subgrids of 30 nodes each are coupled in a ring-like structure (see Figure 2a and Ref. [33] for details). Intuitively, the links between the individual subgrids are most critical for the flows traversing the system. In case of failure, the inter-grid links will have an effect not only on the flow distribution inside the sub-grids but more importantly on the other inter-grid couplings, since all the flow that went through a particular inter-grid link would have to be 're-routed'. Such a failure might thus lead to an overloading of another distant inter-grid link—a *non-local* effect that does not follow trivially from the

¶ This follows directly from the interpretation of the resistance distance in terms of spanning trees, see Ref. [10].

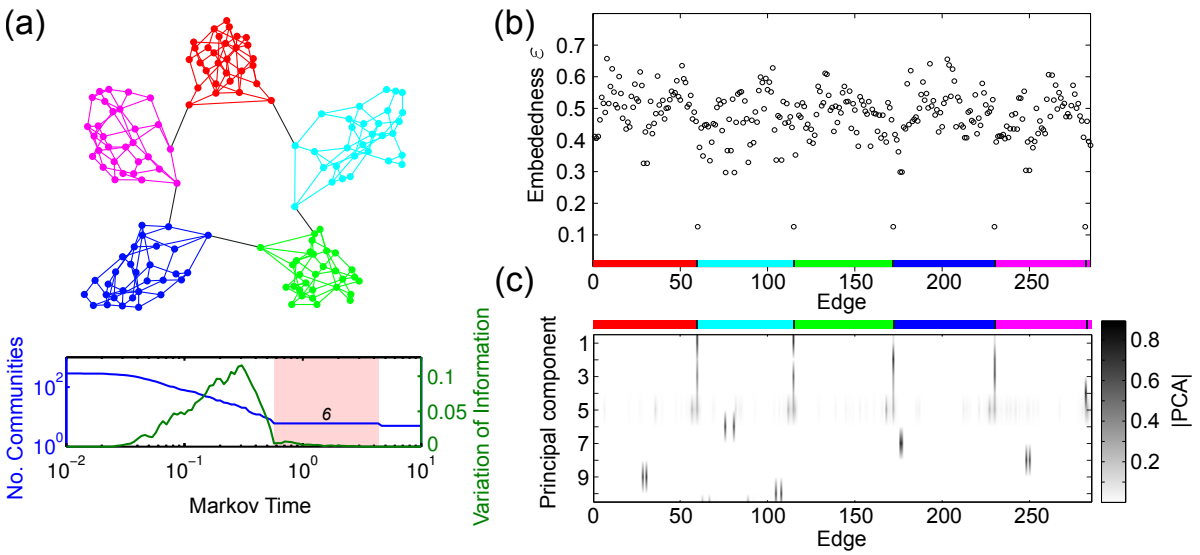


**Figure 2.** Edge-to-edge analysis of a ring of small-worlds. (a) The network analyzed with edges coloured according to the community structure found in the flow-redistribution matrix using the Markov stability method [30, 32]. The partition into 6 communities is stable over a long span of the Markov times with vanishing variation of information, thus signalling its robustness. (b) Embeddedness of the edges in the network. (c) Heat map of the first ten PCA components of the flow-redistribution matrix. Note that the edges linking the small-worlds: are grouped together in one community in (a); have low embeddedness in (b); and concentrate a large weight of the dominant principal components in (c).

pattern of immediate node adjacencies. In power grids, the significance of this event is obvious: an overloading of another line might in turn lead to another line failure possibly resulting in a rapid cascade of failures and a blackout of the system.

This intuitive picture can be captured quantitatively with our analysis, as shown in Figure 2. Figure 2b shows that the links between the sub-grids show the smallest values of embeddedness in the network, as expected. Furthermore, we extract the edge-to-edge influences by analysing the community structure of the weighted, directed adjacency matrix constructed from the absolute values of the flow-redistribution matrix (with removed diagonal). To this matrix, we apply the algorithm for Markov stability of graph communities [30–32] in order to detect communities of edges in the graph.

We find a robust partition into six communities: 5 communities correspond to the subgrids, while all the links between subgrids are grouped into one community (Figure 2a). As one might expect, edges within a subgrid are clustered together, as their influence is mostly constrained to their local subgrid. The fact that the inter-grid links form one community means that their influence on each other is very strong. These edges also possess a relatively strong influence on the adjacent subgrids (as they can 'disconnect' them) but their relative influence on each other is even stronger. In fact, the magnitude of the line outage distribution factor between two of these edges is exactly one, indicating that in case of line failure the other inter-grid edges would

be maximally affected. The use of community detection in combination with the flow-redistribution matrix thus reveals *non-local* properties of the network. In the context of power grids, discovering such structural features could complement percolation-based node-centric analyses (e.g. Ref. [36]) and provide input to load-flow based cascading failure models [37].

The above picture based on community analysis is confirmed through a principal component analysis (PCA) of the flow-redistribution matrix (Figure 2c). As discussed above, the range of the flow-redistribution matrix (and hence its principal components) lie in the weighted cut space of the graph. Therefore, PCA reveals the most important weighted cuts in the network with respect to flow redistribution. Figure 2c shows that the first principal components only have components involving the inter-subgrid couplings, confirming the results of our community detection analysis. In all the examples below, we have carried out a systematic evaluation of the PCA components (not shown), which similarly confirm the results obtained with the edge embeddedness and Markov stability community detection.

## 5. Applications to real-world networks

We now consider several real-world examples. It is important to remark that our aim here is not to perform an in-depth analysis of each of these systems, which would be beyond the scope of this paper, but rather to highlight different aspects of the analysis based on the edge-to-edge measures introduced above.

### *5.1. The Iberian Power Grid*

The first example we consider is the Iberian subnet of the European Power Grid [33, 39, 40], which consists of 403 nodes corresponding to generators and substations and 622 edges representing high-voltage transmission lines. Beyond ascertaining the $N-1$ robustness against failure propagation [26], here we use the measures derived above to carry out a network-theoretic analysis of this power grid revealing (non local) edge-to-edge features. We remark that our description of power systems as resistor networks corresponds to adopting the so-called DC power flow approximation, a common representation in which the non-linear load-flow equations are linearised around a reference state.

Using Markov stability for community detection as discussed above, we find that one of the most relevant partitions splits the edges of the network into three main communities, as shown in Figure 3a-b. Interestingly, this partition uncovers non-local relationships between the edges: the transmission lines that connect the north-east with the central part of the grid (edges c1-c3 in Figure 3b), roughly going from Saragossa towards Madrid, appear to be strongly linked to the north-western part of the grid and form part of this community (green). Figure 3c confirms this finding: the influence of edges c1-c3 are much more significant on the north-west (green) community. This

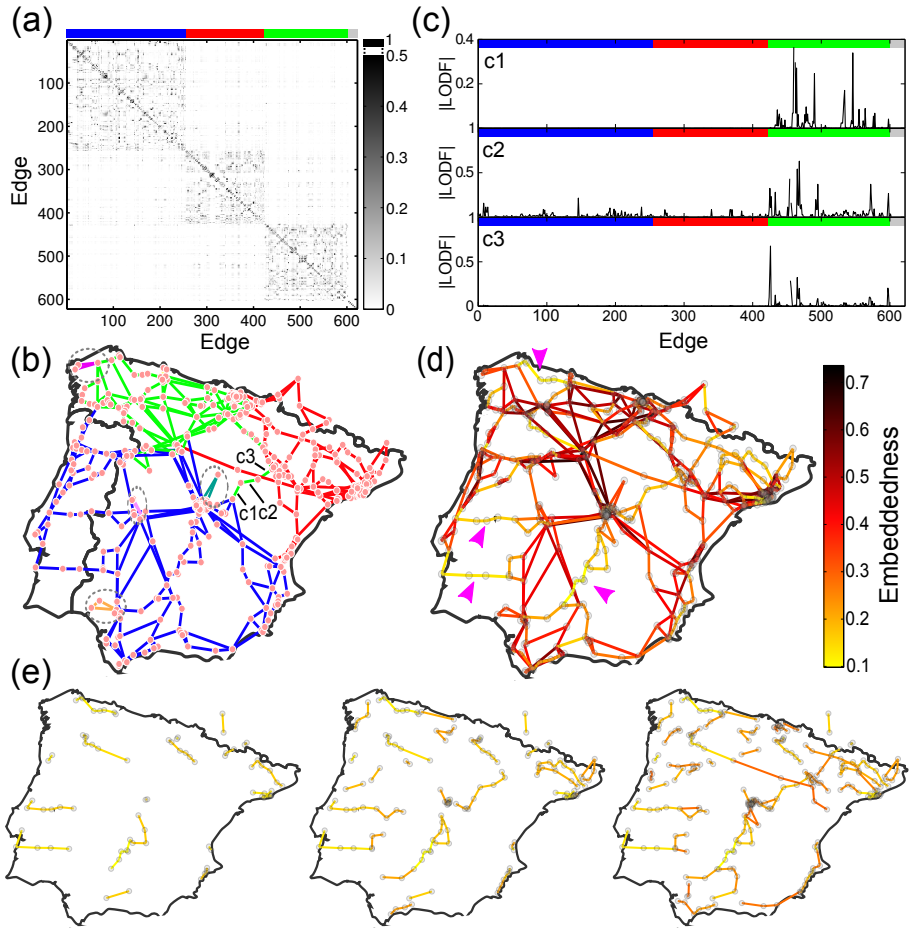


**Figure 3.** Analysis of the Iberian Power Grid. (a) flow-redistribution matrix ordered according to the community structure found with the Markov stability method. (b) Map of the Iberian Power Grid with colours denoting edge communities. The community structure displays *non-local* structure: the edges c1–c3 are grouped with the north-west (green) community, although these edges lie between the north-east (red) and central-south (blue) communities and have no direct connection with the north-west (green) community. Small local circles (encircled with gray dotted lines), form their own isolated communities, i.e., they are effectively 'decoupled' from the rest of the network. (c) Influence of edges c1–c3 on all other edges in the network as measured by the magnitude of the line outage distribution factor (LODF). (d) Edge embeddedness of all the edges in the network. There are several weakly embedded paths of lines (marked with magenta arrows), e.g., those connecting the center and south of Portugal with Spain; the lines going from the centre to the south, from Madrid towards Andalusia; or the lines connecting Asturias and Galicia along the North-Northwest coast [38]. (e) Weakly embedded edges in the Iberian Power Grid. From left to right, the lowest 10%, 20% and 35% embedded edges and associated nodes.

behaviour emerges from the fact that edges c1-c3 are part of a long loop going from the northwest eastwards; connecting to the center via a southern branch containing edges c1-c3; and eventually going back to the northwest.

The sensitivity of the flow-redistribution matrix in detecting the importance of such alternative cyclic paths also underlies the detection of several small 'triangle-

type communities' (encircled in dashed lines in Figure 3b), which are 'decoupled' flow-wise from the rest of the network, i.e. the links within these small communities only participate in a single cycle in the whole network.

An analysis of the embeddedness of the edges in the Iberian grid is shown in Figure 3d-e. As we might expect from our previous analysis, edges c1-c3 are only weakly embedded in the graph. In fact, their embeddedness is even smaller than that of the 'triangle-type communities' mentioned above, although c1-c3 are part of more than one cycle. Note also that the lines connecting the center and south of Portugal with Spain show very small embeddedness due to the lack of alternative routes. A similar observation applies to the line leading from Madrid towards the south and the line connecting Asturias and Galicia in the Northwest coast. All of these lines are indicated with magenta arrows in Figure 3d. Interestingly, several of these lines are associated with relatively new solar plants, as can be seen in [38]. An additional assessment of the importance of the individual lines is shown in Figure 3e, in which the weakly embedded lines of the Iberian grid are displayed.

### *5.2. Traffic networks*

As a second example, we consider traffic networks corresponding to parts of the street networks of London, Boston and New York [41]. We analyze the networks reported in Ref. [41] (data kindly provided by H. Youn), in which the nodes correspond to street intersections and the edges are principal roads as classified by Google Maps. In our analysis we assume the streets to be undirected and the edge weights correspond to the number of street lanes. In these systems, currents can be naturally identified with traffic flows and voltages with delays, although the relationship between flows and delays is in general non linear (see [41] and references therein). Hence, our analogy with a linear resistor network amounts to assuming a socially optimal behaviour for all drivers, and in particular "Braess paradox" [41, 42] cannot arise in our context. However, based on our simplified linear model, we use the flow-redistribution matrix and related measures to perform a coarser, topological analysis of traffic flows independent of patterns of injected flow. We can thus assess the relative interdependence and importance of the edges (roads) with respect to any (linear) traffic flow, rather than focussing on the influence of an edge for a particular source-target pair.

Figure 4 displays the results of our community detection algorithm on these street networks based on the edge-to-edge flow-redistribution matrix. In the case of London, we find a relevant partition into nine communities of streets, eight of which correspond to well delimited city areas while the ninth is a non-local community of edges comprising two alternative main north-south routes across the Thames: Waterloo Bridge and Farringdon Street, which is a continuation of Blackfriars Bridge. Our analysis indicates that these two routes are therefore strongly coupled in terms of flow redistribution. For the two American cities, such non-local community structure is not observed, as could be expected given the more regular, grid-like structure of both networks. In

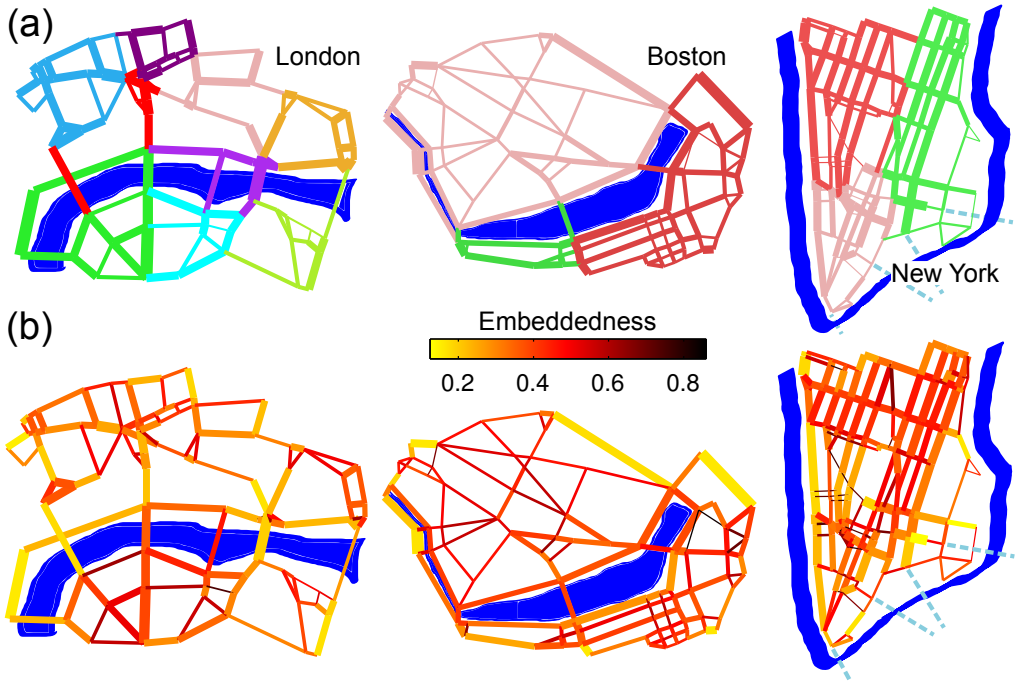


**Figure 4.** Analysis of Urban Street Networks of London (82 nodes, 217 edges), Boston (88 nodes, 155 edges), and New York (125 Nodes; 215 edges). Nodes correspond to intersections and edges to (undirected) streets weighted according to the number of lanes. Light blue dashed lines indicate some connecting roads not part of the analyzed network. (a) Communities of streets (denoted by different colours) found from the analysis of the flow-redistribution matrix with the Markov stability method. The streets within each community have a strong influence on each other. Unlike Boston and New York, we detect non-local community structure in the streets of London (red community). (b) Embeddedness of the edges in the street networks. The mean embeddedness in London, $\langle\varepsilon\rangle_{\text{London}} = 0.377$, is lower than for the US cities ($\langle\varepsilon\rangle_{\text{Boston}} = 0.439, \langle\varepsilon\rangle_{\text{NewYork}} = 0.429$), mainly due to the more grid-like structure of the principal roads in the US street networks. Note the low embeddedness of most bridges (or continuation streets) in London and the existence of a core of highly embedded streets at the centre of Lower Manhattan.

the case of New York, we obtain a relevant partition into three communities of streets corresponding approximately to Lower Manhattan/Financial district in the south; Kips Bay/Lower East Side/East Village on the East side; and Greenwich Village/Chelsea on the West side. Similarly, Boston is split into three communities of streets corresponding to Back Bay/Downtown/Beacon Hill; a second community extending over Cambridge; and a third, smaller community comprising the Boston University area and Harvard Bridge over the Charles.

The study of the edge embeddedness reveals further differences between the cities. In particular, London and New York present the most dissimilar profiles of $\boldsymbol{\varepsilon}$: London has the lowest mean embeddedness with a significant tail of streets with low $\varepsilon$, while New York has the broadest distribution of $\varepsilon$. The edge embeddedness in New York markedly increases as we go towards Chinatown/Little Italy/Canal Street, where we

find a central core of highly embedded streets. This is expected from the grid-like structure of the street network one typically encounters in American cities, which by construction provides many alternative paths to most locations in the network. New York also has a set of streets with low embeddedness mostly in the periphery. The presence of low $\varepsilon$ edges at the boundaries of the graph is expected since the flows at the boundaries have fewer alternative paths to be redistributed. Studying the relevance of such low peripheral $\varepsilon$ on larger street networks that have not been artificially 'cropped' will be the subject of future work. Interestingly, the presence of 'internal boundaries' can also induce low edge embeddedness. An example for such a street with low $\varepsilon$ is the Lincoln Highway/West Street on West Lower Manhattan, which has the Hudson River as a natural boundary. In the case of London, a significant fraction of the streets with low $\varepsilon$ lies in the north-south direction, connecting the areas south of the river Thames with the northern part of the network. Most of these roads correspond to bridges, which are bottlenecks in the real street network. In fact, all but one bridge have $\varepsilon$ below the mean, including Waterloo Bridge, London Bridge and Westminster Bridge with particularly low scores. The street network of Boston shows a less extreme grid-like structure than that of New York and falls therefore somewhere in between London and New York (see Figure 4).

### *5.3. Neuronal network of C. Elegans*

Our final example is the neural network of the worm *C. elegans*, one of the few model organisms for which the entire neural wiring is almost completely available. Here we use the strongly connected giant component of the network of gap junctions and chemical synapses (recently enlarged and curated by [43]), which consists of 274 nodes (neurons) and 2253 edges (synapses and gap junctions) [44], which we assume to be undirected. We reiterate that an in-depth analysis of the functional and structural features of this neuronal network is beyond the scope of this paper. For pointers to the vast and comprehensive literature on the subject, see, e.g., [43, 45, 46] and references therein.

In order to display and interpret our results, we use the classification of neurons into body compartments and functional types found at http://www.wormatlas.org/neuronalwiring.html [43]. Position-wise, edges are denoted according to the compartment (head: H, mid-body: B, or tail: T) in which its end points lie, e.g., an HB edge connects the head and mid-body regions. Type-wise, edges are denoted according to the type of neuron (sensory ($\mathcal{S}$), interneuron ($\mathcal{I}$) and motor ($\mathcal{M}$)) that they connect, e.g., a $\mathcal{S}$-$\mathcal{I}$ edge connects a sensory neuron to a motor neuron.

In Figure 5a-b, we show the eight communities of edges (denoted by different colours) of this neuronal network, as obtained by analysing the flow-redistribution matrix with Markov stability community detection. Figure 5a shows the communities of synapses ordered according to body positions. As expected, the edge communities are closely linked to the body structure of the worm. More precisely, the communities are mainly centered around either head, mid-body, or tail positions, i.e. the core of

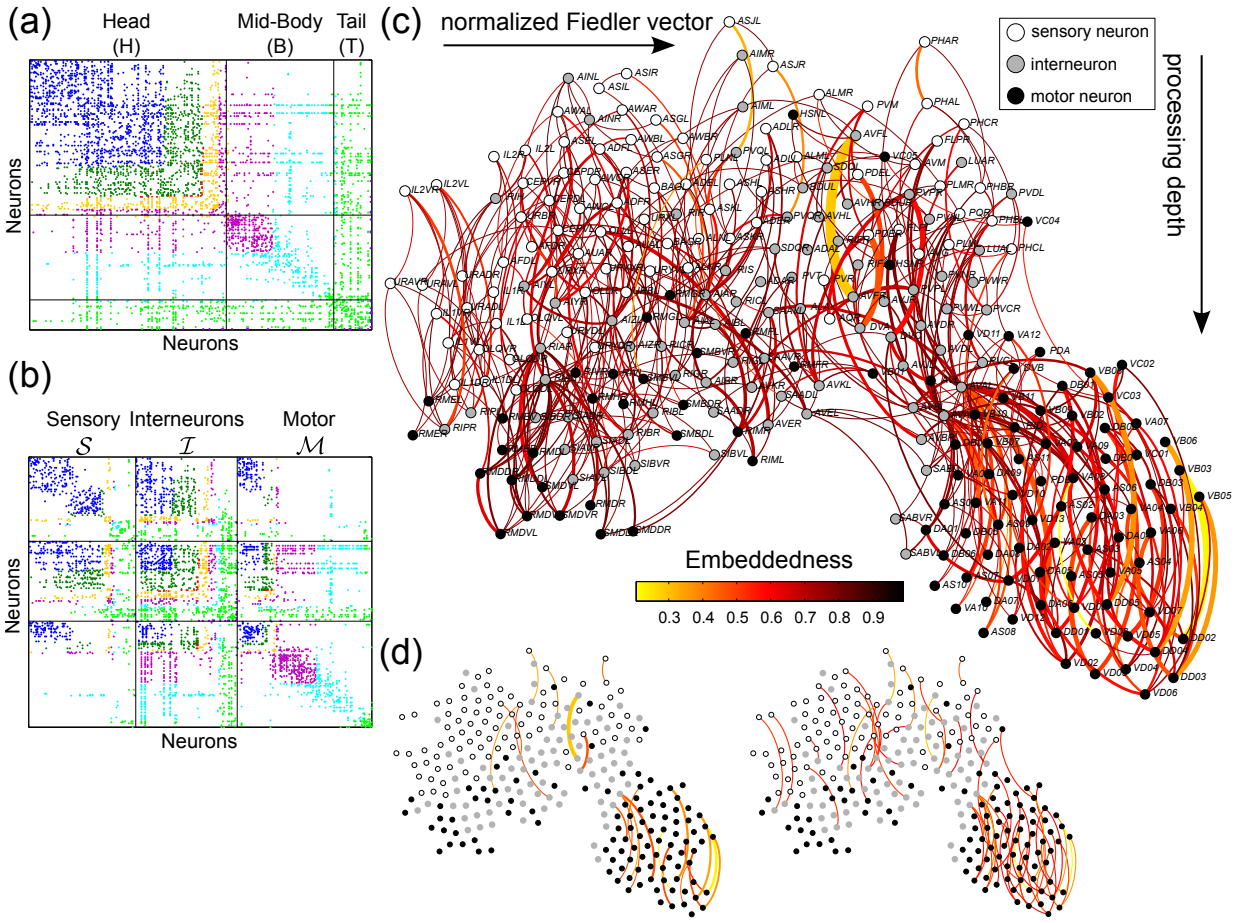


**Figure 5.** Analysis of the neural network of *C. elegans*. The edges of this network (synapses and gap junctions) were found to belong to 8 robust communities (denoted by different colours in (a) and (b)) according to the analysis of the flow-redistribution matrix using the Markov stability method. (a) Visualisation of the edge communities in the adjacency matrix ordered according to body position (anteroposterior order). (b) Visualisation of the edge communities in the adjacency matrix ordered according to functional categories: sensory neurons $\mathcal{S}$, interneurons $\mathcal{I}$ and motor neurons $\mathcal{M}$. An anteroposterior ordering is applied within each group. (c) Embeddedness of the edges in the *C. elegans* neural network. Neurons are coloured according to type: sensory neurons (white), interneurons (gray), and motor neurons (black). For the visualisation of the network we used the planar display suggested in Ref. [43]: vertical axis corresponds to the position of the neuron in the signaling pathway ( sensory neurons tend to be at the top, motor neurons at the bottom); horizontal axis is the normalised Fiedler vector (which tends to group nodes with more connections to each other closer in space). In this visualisation, we see that the embeddedness grows as the processing depth increases: synapses between sensory neurons (upstream) tend to be more embedded, while edges linked to motor neurons (downstream) tend to be less embedded. (d) This observation is also confirmed by the skeleton of weakly embedded edges in the neuronal network of *C. elegans*: the connections with the lowest 1% (left) and 3% (right) edge embeddedness.

each community comprises a group of either HH, BB, or TT edges. Interestingly, the edges linking different regions tend to belong to communities centered around the region

closest to the tail, e.g., HB edges tend to belong to body-centered communities, while HT edges belong to tail-centered communities (Figure 5a). This indicates a 'downstream' organisation in the way that synaptic changes affect other neurons: a synaptic failure will tend to cascade 'downstream' from the head region, where most sensory neurons lie, towards the body and tail regions, where most interneurons and motor neurons lie. In this sense, changes in sensory synapses 'upstream' tend not to affect other similar sensory synapses and only affect other synapses downstream.

Figure 5b shows the edge communities displayed in accordance with their associated neuronal types ($\mathcal{S}$, $\mathcal{I}$, $\mathcal{M}$). We find that the two communities of edges connecting to mid-body positioned neurons (magenta and cyan colours) correspond mainly to $\mathcal{M}$-$\mathcal{M}$ or $\mathcal{I}$-$\mathcal{M}$ edges. Hence these communities might be thought of as 'downstream' executive communities. On the other hand, the tail-centered community (light green) and one of the head communities (dark green) comprise mostly couplings from interneurons (of all types $\mathcal{S}$-$\mathcal{I}$, $\mathcal{I}$-$\mathcal{I}$, $\mathcal{I}$-$\mathcal{M}$), suggesting a key role of these edges, in agreement with the commonly accepted role of interneurons as controlling units in the neural circuitry. The edge community (blue) with the strongest impact on the sensory modalities includes connections to all neuron types. In particular, the interneurons linked by the $\mathcal{I}$-$\mathcal{I}$ edges in this blue community appear to have a central position in the network: they link from/to any edge community and neuron type, including a large number of connections to motor neurons. One may thus hypothesise that this group of interneurons interconnected by the $\mathcal{I}$-$\mathcal{I}$ edges in the blue community acts as a control hub processing the inputs from sensory neurons and relaying it to motor neurons.

The edge embeddedness of the connections in the neuronal network of *C. elegans* is shown in Figure 5c-d. We find that the edge embeddedness decreases as the processing depth increases, i.e., edges with low embeddedness are predominantly located downstream, in the late stages of the processing hierarchy and connected to motor neurons (see Figures 5d). This can be explained by the fact that motor neurons are essentially terminal nodes activated from upstream processing via only a few connections and, in this sense, they belong to weakly embedded 'pathways'. On the other hand, further up in the signaling chain (in synapses related to sensory neurons), very few edges have low embeddedness (Figure 5d) indicating that signalling synapses are embedded in 'circuits' with more alternative paths. One notable exception is the connection between the AVFL and AVFR interneurons, which shows low embeddedness even if it is high up in terms of processing depth. This low embeddedness reflects a lack of alternative paths for flow redistribution if this synapse fails. Interestingly, the AVFL and AVFR neurons are thought to be involved as decision-making interneurons in the temporal coordination of egg-laying and locomotion of the nematode [47].

## 6. Discussion

Analytical tools used to investigate complex networks have commonly adopted a node-centric perspective, aiming at the characterisation of individual nodes or of groups of

nodes and their relations to each other. In this paper, we have presented tools to characterise edge-to-edge relations inspired by the redistribution of flow induced by line failures. We have shown that the flow-redistribution matrix is a topological descriptor of the network that can be used to quantify edge-to-edge relations induced by flow redistribution. The flow-redistribution matrix can be decomposed into an edge-to-edge transfer function matrix, which describes how much the injection of flow at an edge translates in changes of flow in other edges, and a vector of edge embeddednesses, which describes how costly it is to transit between the two endpoints of each edge through alternative paths in the network. Our analysis provides us with explicit network-theoretic interpretations of these edge-to-edge measures. Adopting such an edge-based perspective can thus provide a complementary view of network properties and allows for a natural detection of structural features which may not be readily found by node-centric methods.

Importantly, the flow-redistribution matrix and the associated edge-to-edge transfer function matrix and embedddedness vector $\boldsymbol{\varepsilon}$ take into account non-local properties of the graph and go beyond local adjacency relations between edges, as represented by the line graph [8, 9]. This fundamentally non-local nature of our measures emanates from the fact that their graph theoretical description is underpinned by the pseudoinverse of the Laplacian. The pseudoinverse of the Laplacian incorporates global properties of the graph and serves to link our measures to other (graph) theoretically relevant properties such as the resistance distance, commute and hitting times of random walks as well as graph embeddings. The definition of our measures comes at the price of the (potentially high) computational cost of computing the pseudoinverse. However, there exist fast algorithms to obtain (approximations or exactly) all currents and voltages in the network [19] or alternatively the resistance distances [28], facilitating the analysis of large networks in terms of the flow-redistribution.

The examples presented above highlight how our edge-based measures are able to detect relevant structural features with an impact on the dynamics of the respective systems. In addition, there are other applications in which adopting an edge-based perspective would appear natural. Think for instance of metabolic control analysis applied to chemical reaction networks. An edge-based analysis may also be interesting for the structural analysis of biomolecules, in which the forming and breaking of bonds (edges) may lead to a significantly different organisation of the system [48], or for financial networks, in which the disturbance of financial flows between different actors may have significant effects on different parts of the network.

## Acknowledgments

The authors thank H. Youn for sharing the street network data. MTS acknowledges support from the German National Academic Foundation in the last stages of this work. JL thanks J. Bernasconi for fruitful discussions. SNY and MB acknowledge funding from the UK EPSRC through grant EP/I017267/1 under the *Mathematics Underpinning the*

*Digital Economy* program and from the US Office of Naval Research (ONR).

## Appendix A. Additional Properties of the Edge-to-Edge Transfer Function matrix

In the following, we elaborate on further properties and interpretations of the edge-to-edge transfer function matrix (see also [28]). First, $M$ is a projection (idempotent) matrix: $M^2 = M$. To see this:

$$\begin{aligned} M^2 &= GB^T L^\dagger BGB^T L^\dagger B \\ &= GB^T L^\dagger LL^\dagger B = GB^T L^\dagger B = M, \end{aligned} \tag{A.1}$$

which follows from the definition of the pseudoinverse. Second, all the eigenvalues of M are either zero or one. To prove this, consider the symmetrised matrix $\widetilde{M} = G^{-1/2}MG^{1/2} = G^{1/2}B^T L^\dagger BG^{1/2}$ and use the singular value decomposition of $B$. It is then easy to show that the eigenvalues of $M$ are $(N-1)$ ones and $(E-N+1)$ zeros (see [28] for a different proof of the same results).

We can give a physical interpretation to these results as follows. Since the graph has $N$ nodes and $E$ edges, we know there are $E-(N-1)$ independent cycles spanning the cycle space [7, 16]. Input currents that fall into the cycle space will balance and yield zero output, thus leading to the $E-(N-1)$ zero eigenvalues. Only inputs that lie in the orthogonal complement of the cycle space, the so called cut space [7, 16], will yield a non-zero current output. Let us call the current input orthogonal to the cycle space the effective input. Conservation of flow implies that the effective input can only be redistributed in the network, i.e. the flow across any weighted cut can at most match this input. In particular, the sum of the flows across any set of (weighted) cut vectors forming a basis for the weighted cut space has to be equal to the effective input. This corresponds to the fact that the remaining $N-1$ eigenvectors of $M$ have unit eigenvalues.

## References

[1] Réka Albert and Albert-László Barabsi. Statistical mechanics of complex networks. *Rev. Mod. Phys.*, 74:47–97, Jan 2002.

[2] S. Boccaletti, V. Latora, Y. Moreno, M. Chavez, and D.-U. Hwang. Complex networks: Structure and dynamics. *Physics Reports*, 424(4-5):175 – 308, 2006.

[3] Alex Arenas, Albert Daz-Guilera, Jurgen Kurths, Yamir Moreno, and Changsong Zhou. Synchronization in complex networks. *Physics Reports*, 469(3):93 – 153, 2008.

[4] Satu Elisa Schaeffer. Graph clustering. *Computer Science Review*, 1(1):27 – 64, 2007.

[5] Santo Fortunato. Community detection in graphs. *Physics Reports*, 486(3-5):75 – 174, 2010.

[6] Frank Harary and Robert Z. Norman. Some properties of line digraphs. *Rendiconti del Circolo Matematico di Palermo*, 9:161–168, 1960.

[7] C.D. Godsil and G.F. Royle. *Algebraic Graph Theory*. Graduate Texts in Mathematics Series. Springer New York, 2001.

[8] T. S. Evans and R. Lambiotte. Line graphs, link partitions, and overlapping communities. *Phys. Rev. E*, 80(1):016105, Jul 2009.

[9] Yong-Yeol Ahn, James P. Bagrow, and Sune Lehmann. Link communities reveal multiscale complexity in networks. *Nature*, 466(7307):761–764, June 2010.

[10] P.G. Doyle and J.L. Snell. *Random walks and electric networks*. Carus mathematical monographs. Mathematical Association of America, 1984. open version available at http://www.math.dartmouth.edu/~doyle/.

[11] Bojan Mohar. Laplace eigenvalues of graphsa survey. *Discrete Mathematics*, 109(1-3):171 – 183, 1992.

[12] Bojan Mohar and Martin Juvan. Some applications of Laplace eigenvalues of graphs. In *Graph Symmetry: Algebraic Methods and Applications, volume 497 of NATO ASI Series C*, volume 497, pages 227–275, 1997.

[13] G. Strang. *Introduction to Applied Mathematics*. Wellesley-Cambridge Press, 1986.

[14] M. Barahona, E. Trías, T. P. Orlando, A. E. Duwel, H. S. J. van der Zant, Shinya Watanabe, and S. H. Strogatz. Resonances of dynamical checkerboard states in Josephson arrays with self-inductance. *Phys. Rev. B*, 55:R11989–R11992, May 1997.

[15] Mauricio Barahona and Shinya Watanabe. Row-switched states in two-dimensional underdamped Josephson-junction arrays. *Phys. Rev. B*, 57:10893–10912, May 1998.

[16] Stephen Guattery. Graph Embeddings, Symmetric Real Matrices, and Generalized Inverses. Technical Report NASA/CR-1998-208462, Institute for Computer Applications in Science and Engineering NASA Langley Research Center, 1998.

[17] Tomaso Poggio, Vincent Torre, and Christof Koch. Computational vision and regularization theory. *Nature*, 317(6035):314–319, September 1985.

[18] J. Hutchinson, C. Koch, J. Luo, and C. Mead. Computing motion using analog and binary resistive networks. *Computer*, 21(3):52 –63, march 1988.

[19] F. Wu and B.A. Huberman. Finding communities in linear time: a physics approach. *The European Physical Journal B - Condensed Matter and Complex Systems*, 38:331–338, 2004.

[20] Y. Yuan, G.-B. Stan, L. Shi, M. Barahona, and J. Goncalves. Decentralised minimum-time consensus. *Automatica*, in press(0):–, 2013.

[21] A. Jadbabaie, N. Motee, and M. Barahona. On the stability of the Kuramoto model of coupled nonlinear oscillators. In *Proceedings of the American Control Conference, 2004.*, volume 5, pages 4296 –4301, 2004.

[22] Arpita Ghosh, Stephen Boyd, and Amin Saberi. Minimizing Effective Resistance of a Graph. *SIAM Review*, 50(1):37–66, 2008.

[23] D. J. Klein and M. Randić. Resistance distance. *Journal of Mathematical Chemistry*, 12:81–95, 1993.

[24] D. Aldous and J. Fill. *Reversible Markov Chains and Random Walks on Graphs*. Book in preparation, 2012. available at http://www.stat.berkeley.edu/~aldous/RWG/book.html.

[25] László Lovász. Random walks on graphs - a survey. Technical Report YALEU/DCS/TR-1029, Yale University, Department Computer Science, New Haven CT 06520, May 1994.

[26] A.J. Wood and B.F. Wollenberg. *Power Generation, Operation, and Control*. Wiley-Interscience, New York, 1996.

[27] Carl D. Meyer Jr. Generalized Inversion of Modified Matrices. *SIAM Journal on Applied Mathematics*, 24(3):pp. 315–323, 1973.

[28] Daniel A. Spielman and Nikhil Srivastava. Graph sparsification by effective resistances. In *Proceedings of the 40th annual ACM symposium on Theory of computing*, STOC '08, pages 563–568, New York, NY, USA, 2008. ACM.

[29] J. Lehmann and J. Bernasconi. to be published.

[30] J.-C. Delvenne, S. N. Yaliraki, and M. Barahona. Stability of graph communities across time scales. *Proceedings of the National Academy of Sciences*, 107(29):12755–12760, 2010.

[31] Jean-Charles Delvenne, Michael T. Schaub, Sophia N Yaliraki, and Mauricio Barahona. The stability of a graph partition: A dynamics-based framework for community detection. In Niloy Ganguly, Animesh Mukherjee, Monojit Choudhury, Fernando Peruani, and Bivas Mitra, editors,

*Time Varying Dynamical Networks*. Birkhäuser, Springer, Boston, 2013. to be published.

[32] Renaud Lambiotte, Jean-Charles Delvenne, and Mauricio Barahona. Laplacian Dynamics and Multiscale Modular Structure in Networks. arXiv:0812.1770, Oct 2009.

[33] Michael T. Schaub, Jean-Charles Delvenne, Sophia N. Yaliraki, and Mauricio Barahona. Markov Dynamics as a Zooming Lens for Multiscale Community Detection: Non Clique-Like Communities and the Field-of-View Limit. *PLoS ONE*, 7(2):e32210, February 2012.

[34] Michael T. Schaub, Renaud Lambiotte, and Mauricio Barahona. Encoding dynamics for multiscale community detection: Markov time sweeping for the map equation. *Phys. Rev. E*, 86:026112, Aug 2012.

[35] Duncan J. Watts and Steven H. Strogatz. Collective dynamics of 'small-world' networks. *Nature*, 393(6684):440–442, June 1998.

[36] Charles D. Brummitt, Raissa M. D'Souza, and E. A. Leicht. Suppressing cascades of load in interdependent networks. *Proceedings of the National Academy of Sciences*, 109(12):E680–E689, 2012.

[37] Jörg Lehmann and Jakob Bernasconi. Stochastic load-redistribution model for cascading failure propagation. *Phys. Rev. E*, 81:031129, Mar 2010.

[38] See http://en.wikipedia.org/wiki/List_of_power_stations_in_Spain.

[39] Martí Rosas-Casals, Sergi Valverde, and Ricard V. Solé. Topological Vulnerability of the European Power Grid under Errors and Attacks. *I. J. Bifurcation and Chaos*, 17(7):2465–2475, 2007.

[40] Ricard V. Solé, Martí Rosas-Casals, Bernat Corominas-Murtra, and Sergi Valverde. Robustness of the European power grids under intentional attack. *Phys. Rev. E*, 77(2):026102, Feb 2008.

[41] Hyejin Youn, Michael T. Gastner, and Hawoong Jeong. Price of Anarchy in Transportation Networks: Efficiency and Optimality Control. *Phys. Rev. Lett.*, 101:128701, Sep 2008.

[42] Dirk Witthaut and Marc Timme. Braess's paradox in oscillator networks, desynchronization and power outage. *New Journal of Physics*, 14(8):083036, 2012.

[43] Lav R. Varshney, Beth L. Chen, Eric Paniagua, David H. Hall, and Dmitri B. Chklovskii. Structural Properties of the Caenorhabditis elegans Neuronal Network. *PLoS Comput Biol*, 7(2):e1001066, 02 2011.

[44] The dataset is publicly available under http://web.mit.edu/lrv/www/elegans/.

[45] J. G. White, E. Southgate, J. N. Thomson, and S. Brenner. The Structure of the Nervous System of the Nematode Caenorhabditis elegans. *Philosophical Transactions of the Royal Society of London. B, Biological Sciences*, 314(1165):1–340, 1986.

[46] Yunkyu Sohn, Myung-Kyu Choi, Yong-Yeol Ahn, Junho Lee, and Jaeseung Jeong. Topological Cluster Analysis Reveals the Systemic Organization of the Caenorhabditis elegans Connectome. *PLoS Comput Biol*, 7(5):e1001139, 05 2011.

[47] Laura Anne Hardaker, Emily Singer, Rex Kerr, Guotong Zhou, and William R. Schafer. Serotonin modulates locomotory behavior and coordinates egg-laying and movement in Caenorhabditis elegans. *Journal of Neurobiology*, 49(4):303–313, 2001.

[48] A Delmotte, E W Tate, S N Yaliraki, and M Barahona. Protein multi-scale organization through graph partitioning and robustness analysis: application to the myosinmyosin light chain interaction. *Physical Biology*, 8(5):055010, 2011.